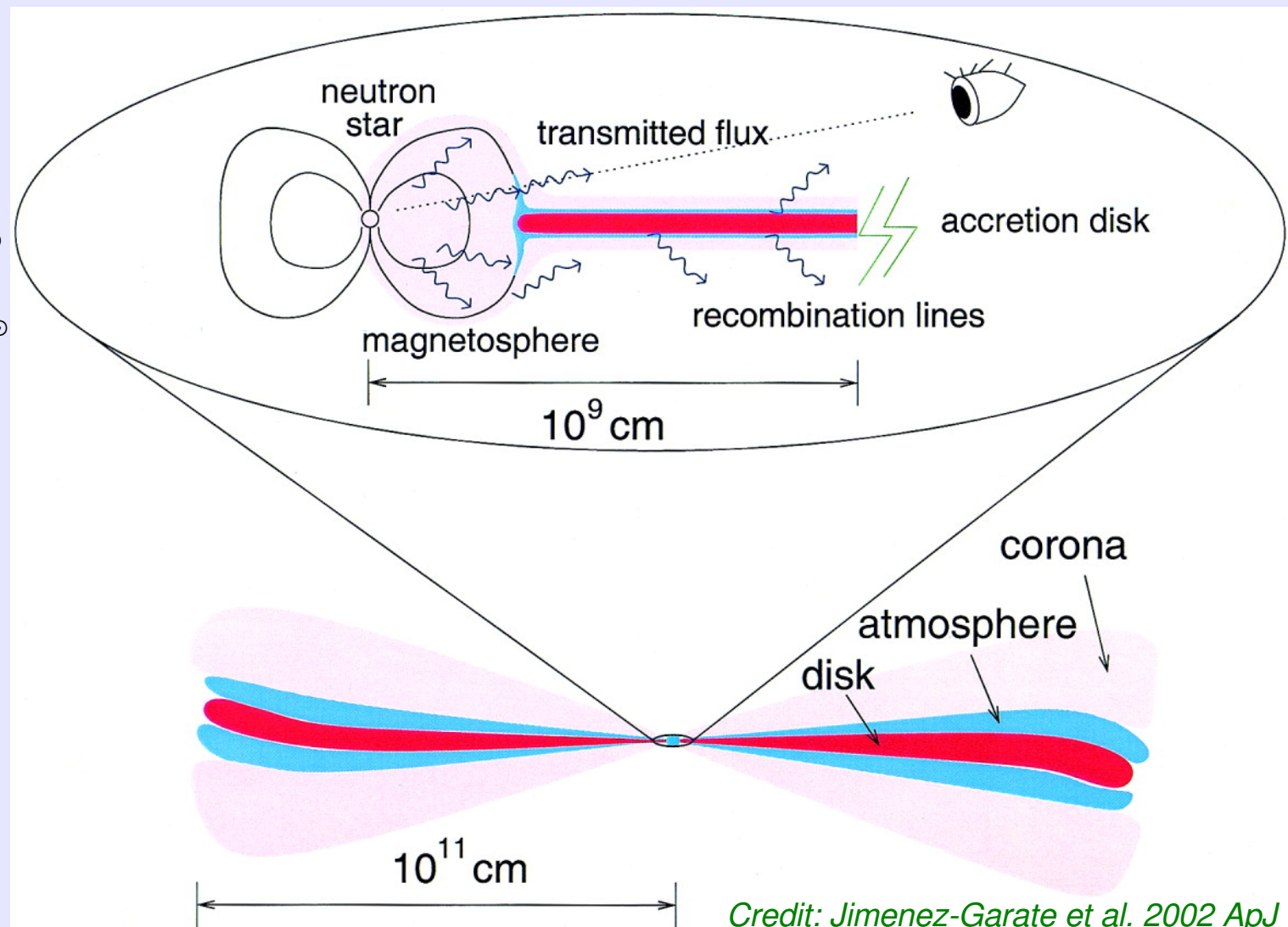


Properties of the Accretion Disk Corona in Her X-1

L. Ji, N. Schulz, M. Nowak & H. Marshall

MIT Kavli Institute for Astrophysics & Space Research

- Neutron star: $1.5 \pm 0.3 M_{\odot}$
- Companion: $2.3 \pm 0.3 M_{\odot}$
- Distance: 6.6 ± 0.4 Kpc
- Disk size: $\sim 1.4 \times 10^{11} cm$
- P_{orb} : 1.7d
- P_{ψ} : ~ 35 d



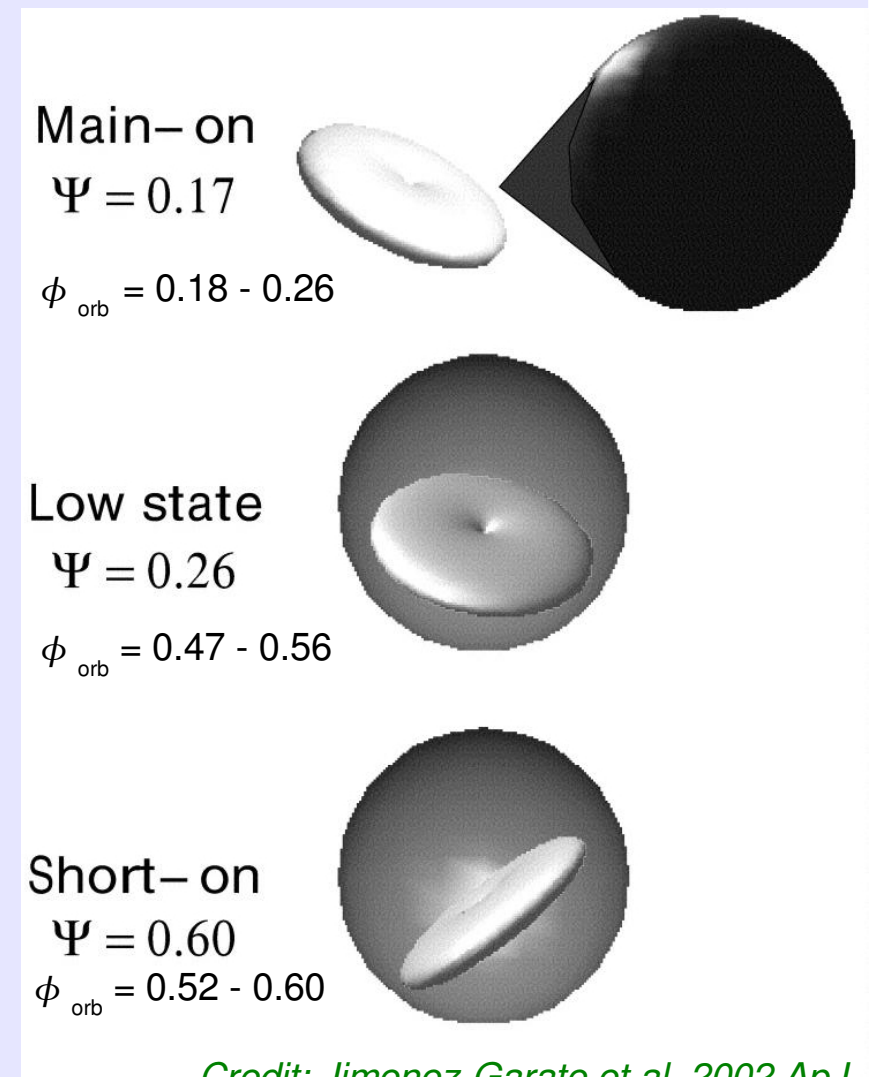
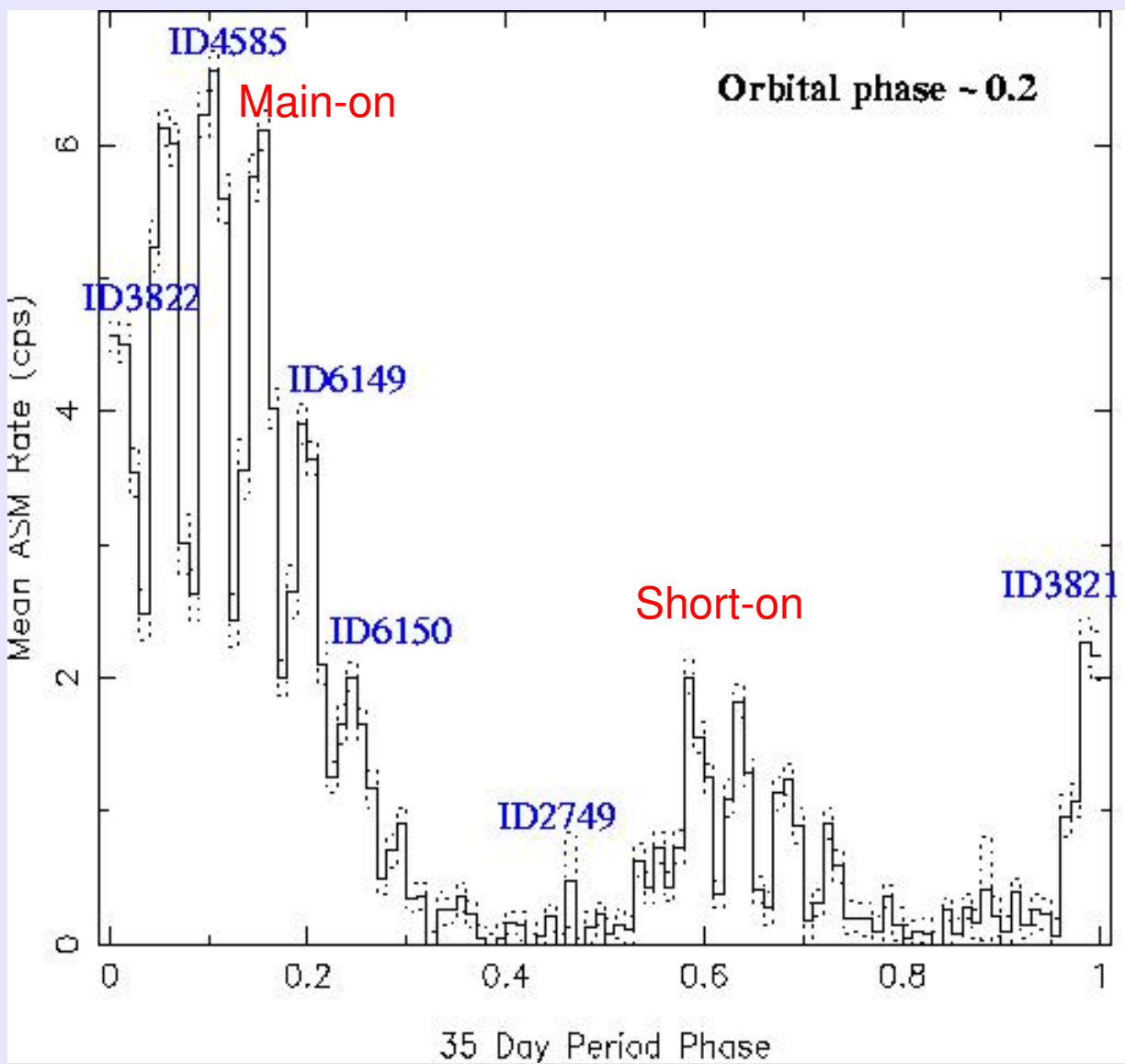
Existing Chandra HETGs Observations

obsID	MJD interval	Observation Start	Exposure(ks)	Orbital phase ^a	35 day Phase ^a
2749	52399.427 - 52400.032	2002-05-05 10:14:49 UT	50.17	0.33 - 0.68	0.42
3821	52875.886 - 52876.261	2003-08-24 21:15:16 UT	30.10	0.57 - 0.79	-0.03
3822	52982.987 - 52983.379	2003-12-09 23:41:44 UT	30.14	0.57 - 0.80	0.04
4585	53335.256 - 53335.512	2004-11-26 06:08:16 UT	20.16	0.76 - 0.91	0.10
6149	53338.630 - 53338.913	2004-11-29 15:06:38 UT	22.14	0.75 - 0.91	0.19
6150	53340.370 - 53340.647	2004-12-01 08:52:39 UT	22.05	0.77 - 0.93	0.24

^aUsing $P_{orb} = 1.700167387$ s at $T_{\pi/2} = 50290.659202$ (MJD) (Private contact from R. Staubert)

- ◆ Total ~ 170 ks
- ◆ Three combinations of orbital and super-orbital phases

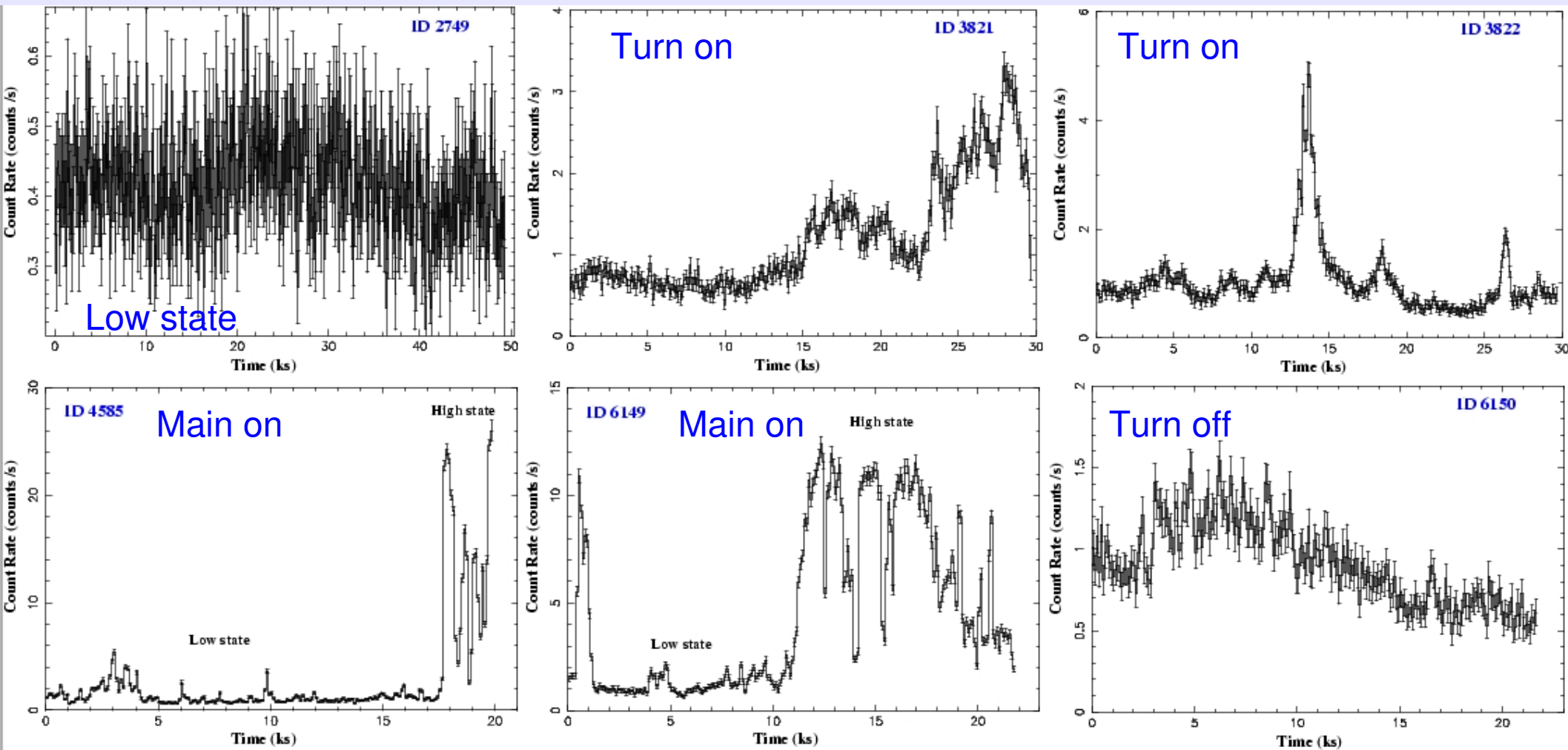
Averaged Light Curve



Credit: Jimenez-Garate et al. 2002 ApJ

- Observations from ASM on board of *RXTE*

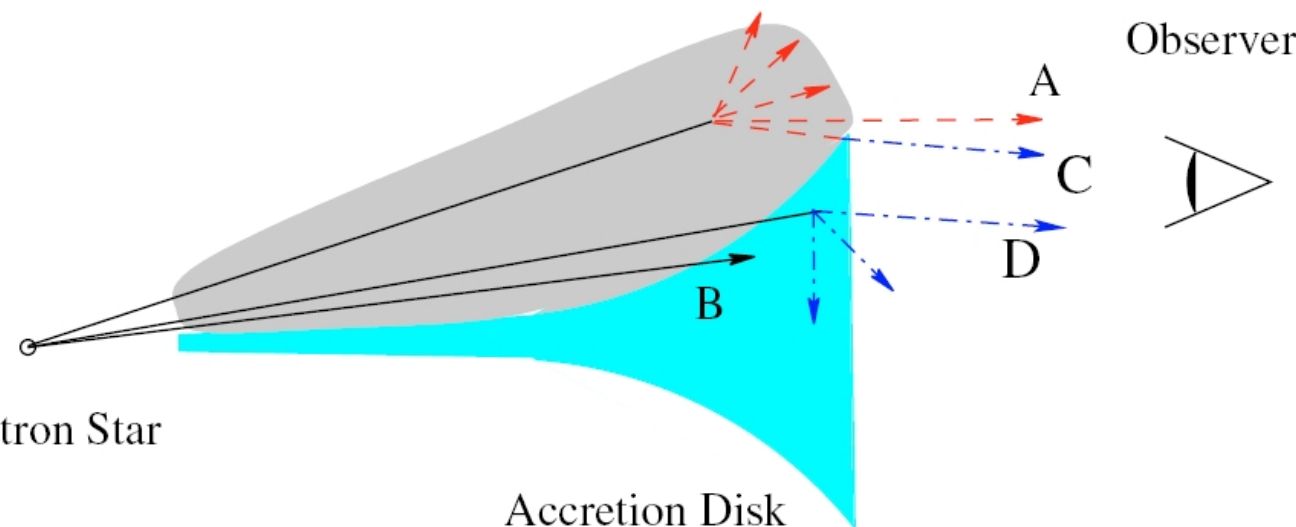
Light Curves for $\lambda > 1.5\text{\AA}$



Continuum Analysis

Schematic illustration of the geometry during turn-on of Her X-1

Accretion Disk Corona



Neutron Star

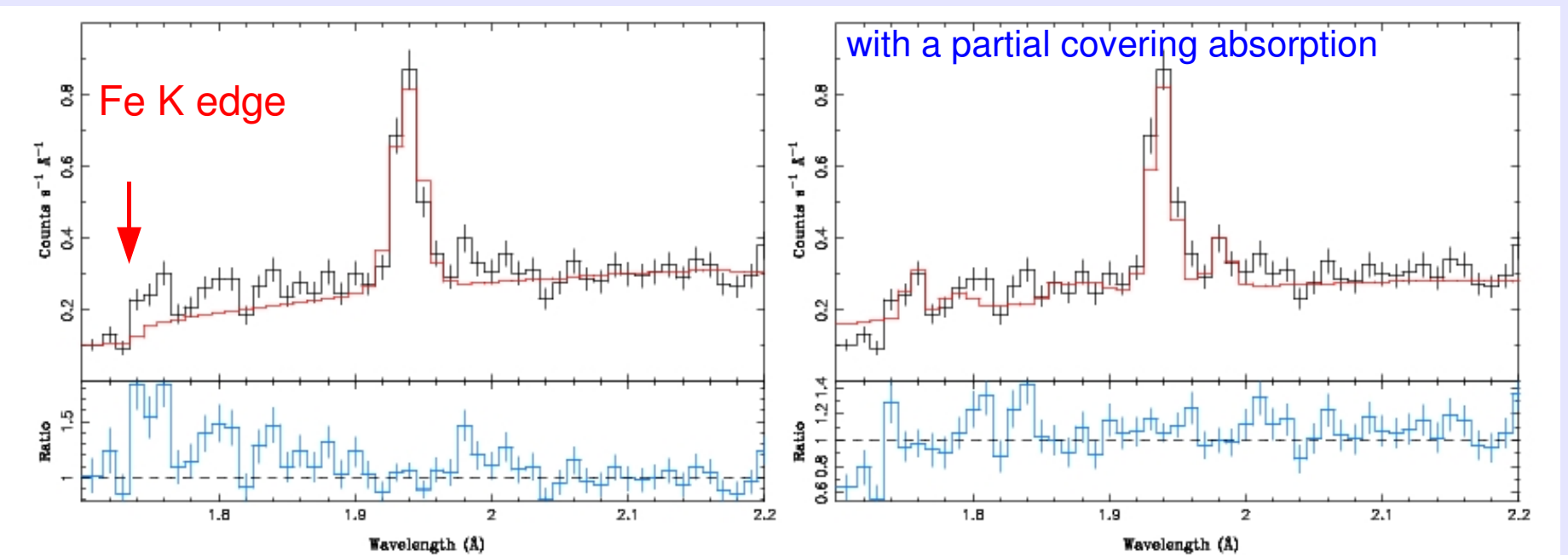
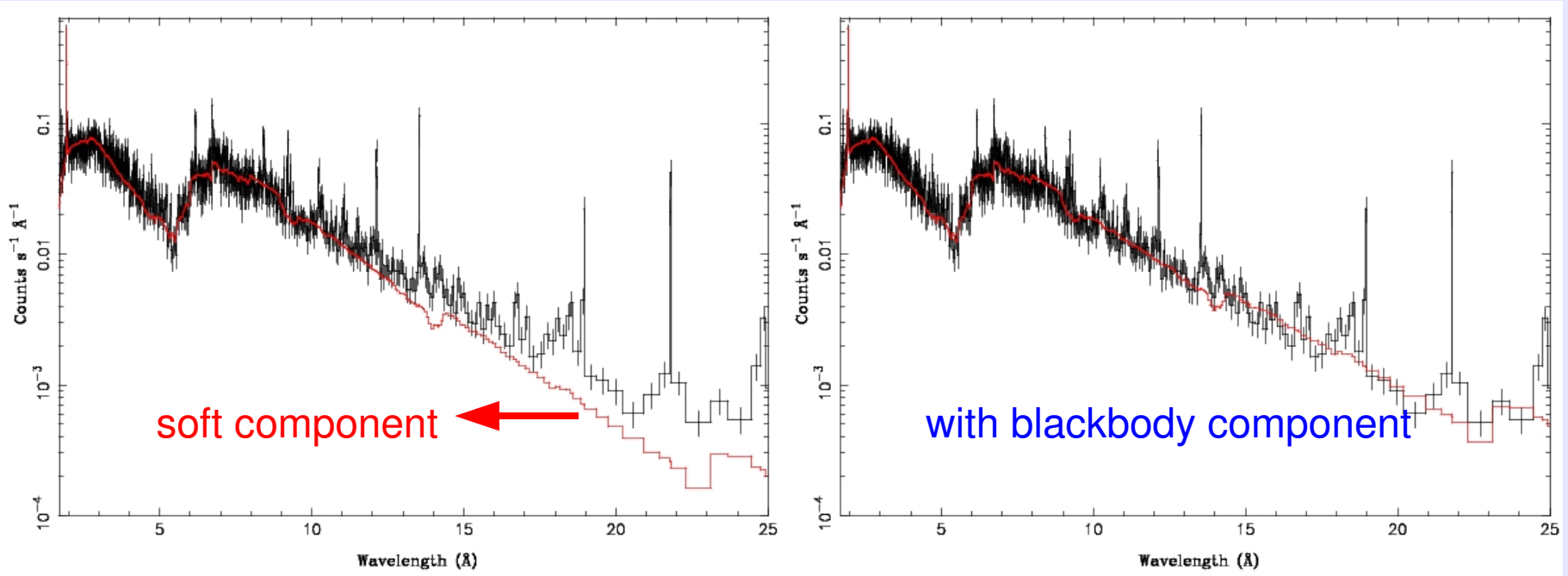
Accretion Disk

Parameter	Value
α	1.068
E_{cutoff}	21.5 keV
E_{fold}	14.1 keV
E_{cyc}	39.4 keV
σ_{cyc}	5.1 keV
E_{Fe}	6.45 keV
σ_{Fe}	0.45 keV

Analysis of RXTE observations shows that the spectra in [3,17] keV can be well described by a partial covering model.

Credit: Kuster et al. A&A 2005

Continuum Analysis



Continuum Analysis Results

obsID	nH 10^{22} cm^{-2}	C	kT (keV)	K1 ^a $10^{39} \text{ ergs s}^{-1}/(10 \text{ kpc})^2$	K2 ^b photons $\text{keV}^{-1} \text{ cm}^{-2} \text{ s}^{-1}$	Cash/dof	Flux ^d
2749	$19.573_{-1.538}^{+1.590}$ ^c	$0.753_{-0.018}^{+0.020}$	$0.129_{-0.012}^{+0.012}$	$1.341_{-0.275}^{+0.353} \times 10^{-4}$	$7.349_{-0.599}^{+0.664} \times 10^{-3}$	1026/598	0.95
3821	$19.307_{-1.336}^{+1.408}$	$0.833_{-0.009}^{+0.008}$	$0.100_{-0.013}^{+0.014}$	$4.810_{-1.574}^{+2.657} \times 10^{-4}$	$3.049_{-0.157}^{+0.167} \times 10^{-2}$	1068/781	3.74
3822	$28.304_{-1.434}^{+1.655}$	$0.907_{-0.005}^{+0.005}$	> 0.052	$> 3.283 \times 10^{-4}$	$4.438_{-0.232}^{+0.268} \times 10^{-2}$	970/673	5.38
4585-H	$29.949_{-0.796}^{+0.832}$	0.95	$0.110_{-0.016}^{+0.015}$	$1.709_{-0.571}^{+1.075} \times 10^{-3}$	$7.929_{-0.176}^{+0.180} \times 10^{-2}$	664/454	10.00
6149-H	$24.642_{-1.433}^{+1.459}$ ^c	$0.884_{-0.010}^{+0.010}$	$0.127_{-0.013}^{+0.014}$	$1.237_{-0.302}^{+0.403} \times 10^{-3}$	$5.805_{-0.489}^{+0.535} \times 10^{-2}$	520/426	7.40
4585-L	$11.254_{-1.127}^{+1.221}$	$0.734_{-0.012}^{+0.012}$	$0.141_{-0.008}^{+0.008}$	$3.521_{-0.416}^{+0.470} \times 10^{-3}$	$1.440_{-0.068}^{+0.073} \times 10^{-1}$	977/795	18.61
6149-L	$10.295_{-0.635}^{+0.998}$	$0.699_{-0.007}^{+0.004}$	$0.136_{-0.004}^{+0.003}$	$3.126_{-0.195}^{+0.246} \times 10^{-3}$	$9.428_{-0.235}^{+0.338} \times 10^{-2}$	1665/1208	12.80
6150	$27.711_{-1.863}^{+2.322}$	$0.897_{-0.007}^{+0.008}$	$0.110_{-0.013}^{+0.014}$	$6.430_{-2.038}^{+3.026} \times 10^{-4}$	$3.581_{-0.235}^{+0.305} \times 10^{-2}$	782/530	4.44

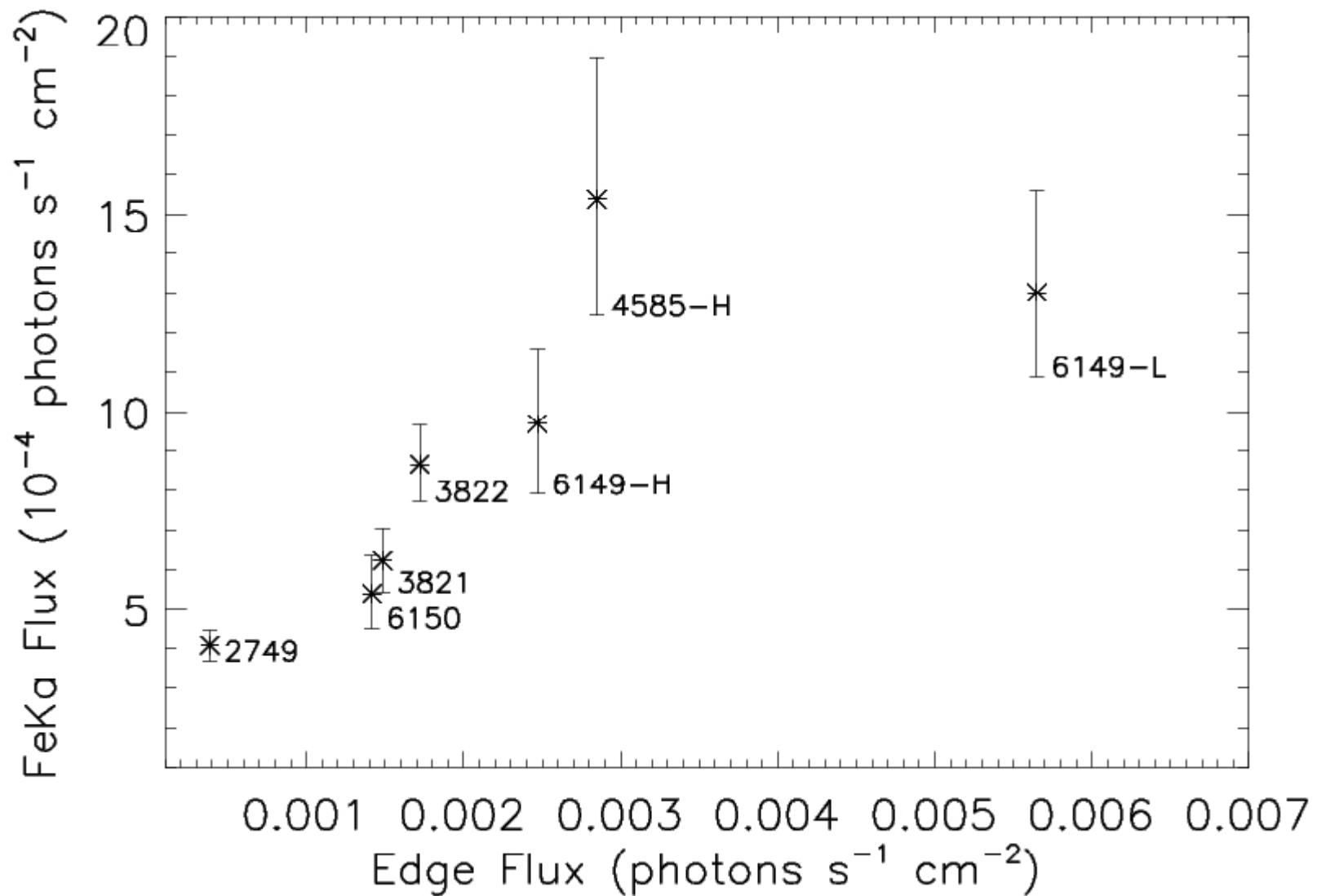
^aNormalization for blackbody component

^bNormalization for cutoff-powerlaw component, where photon index is fixed at 1.068 and high energy cut at 21.5 keV

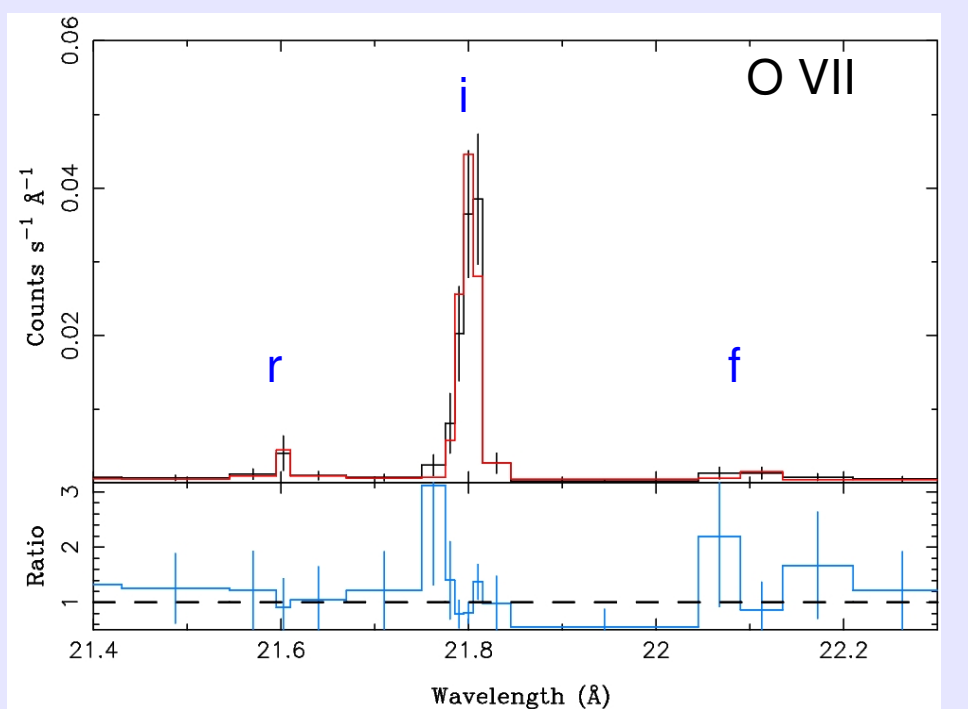
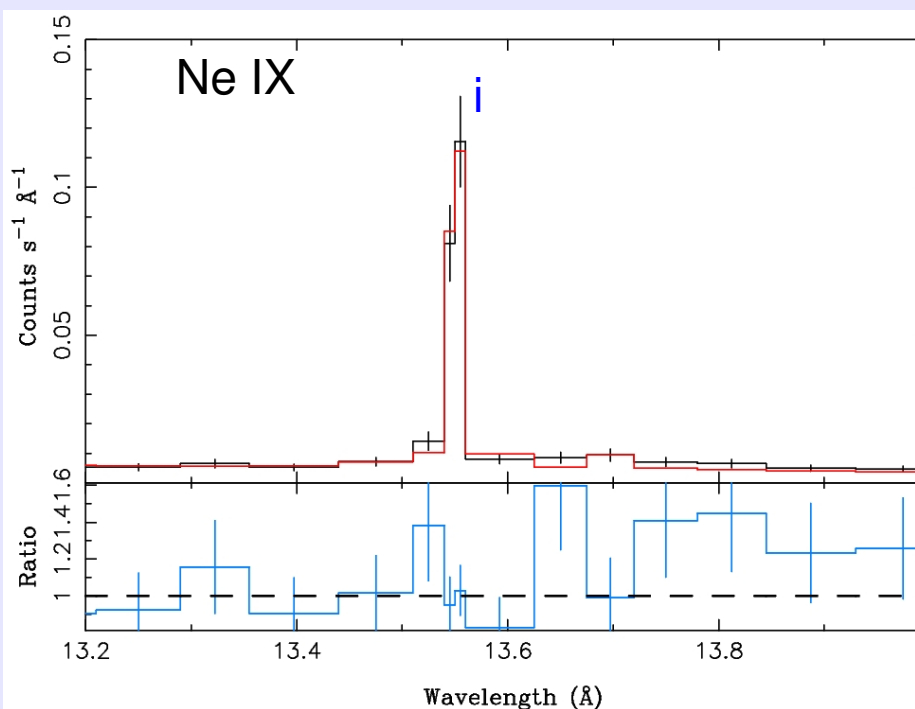
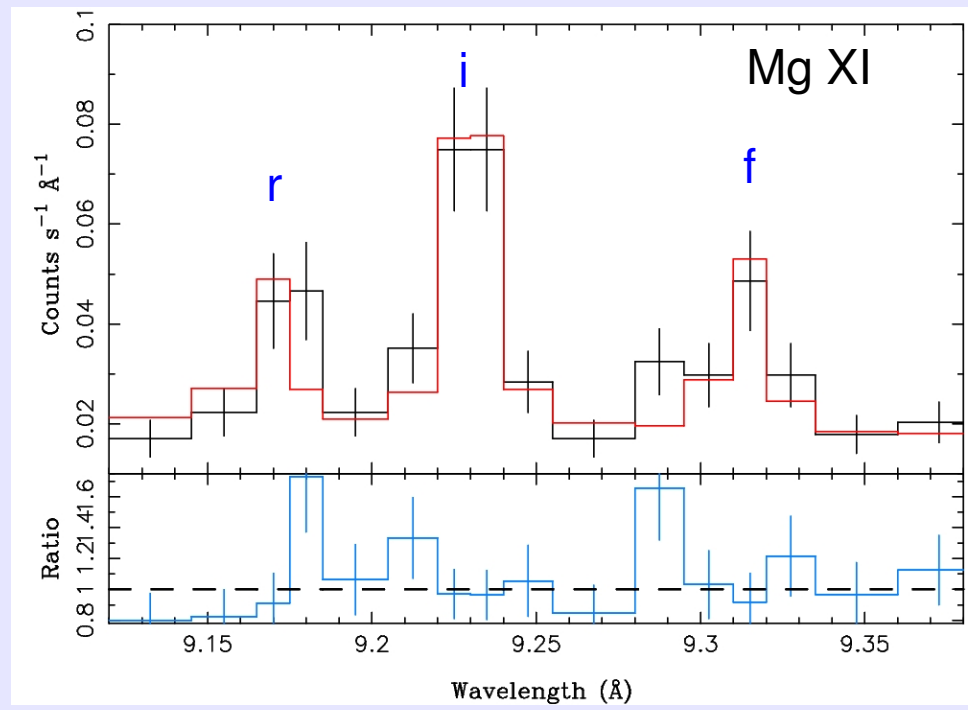
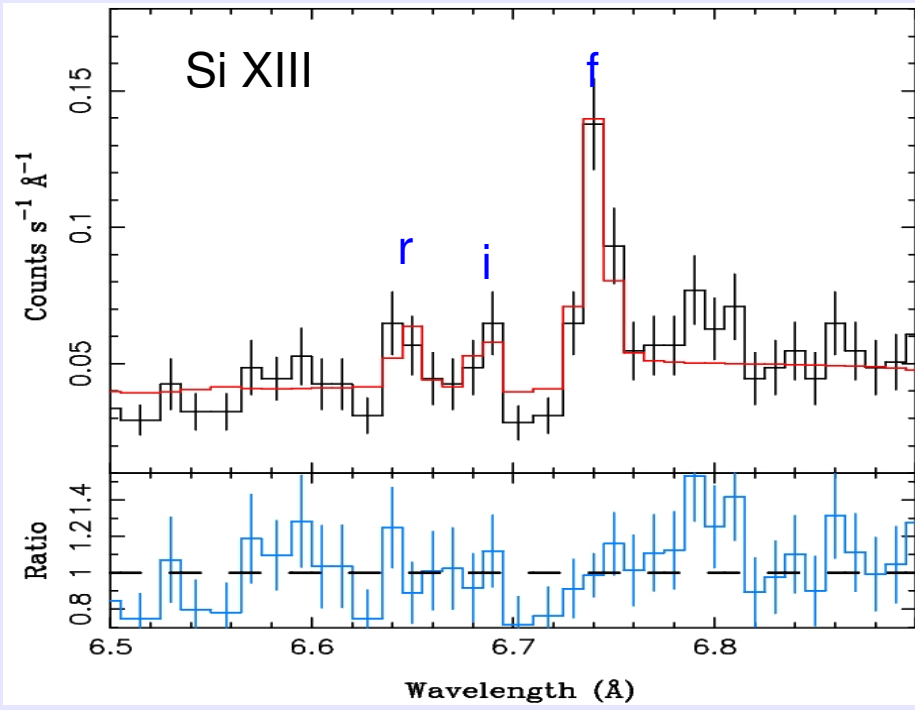
^cat 67% confidence level

^dFlux is in unit of $10^{-10} \text{ ergs s}^{-1} \text{ cm}^{-2}$ and in [0.3,10]keV band

Fluorescence lines Fe K



Helium-like triplet lines

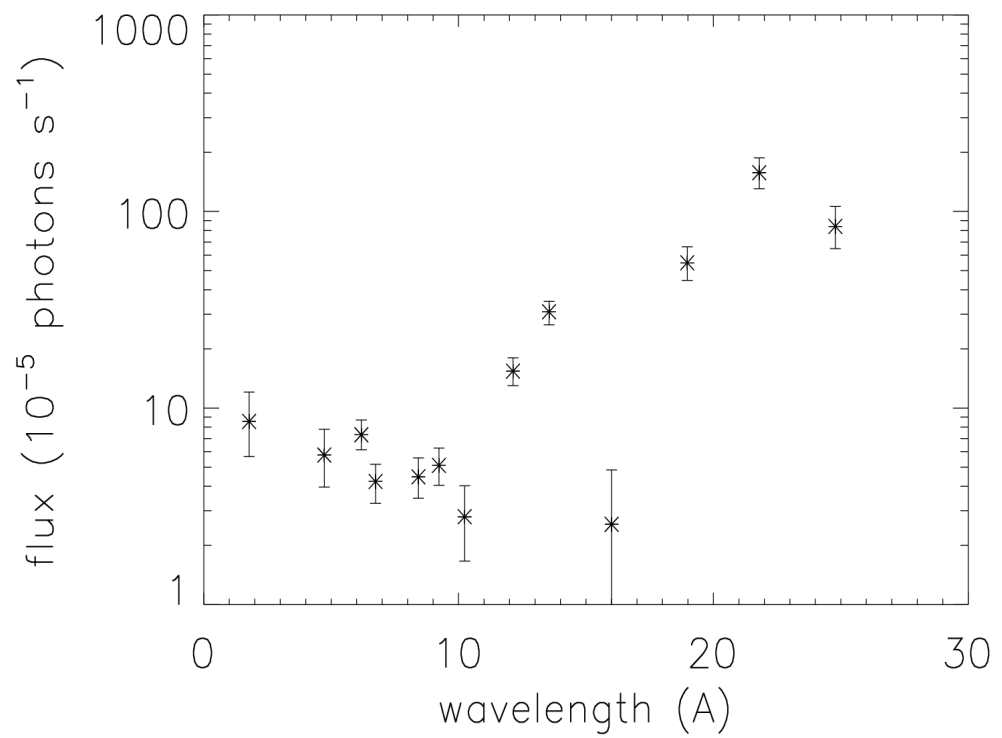
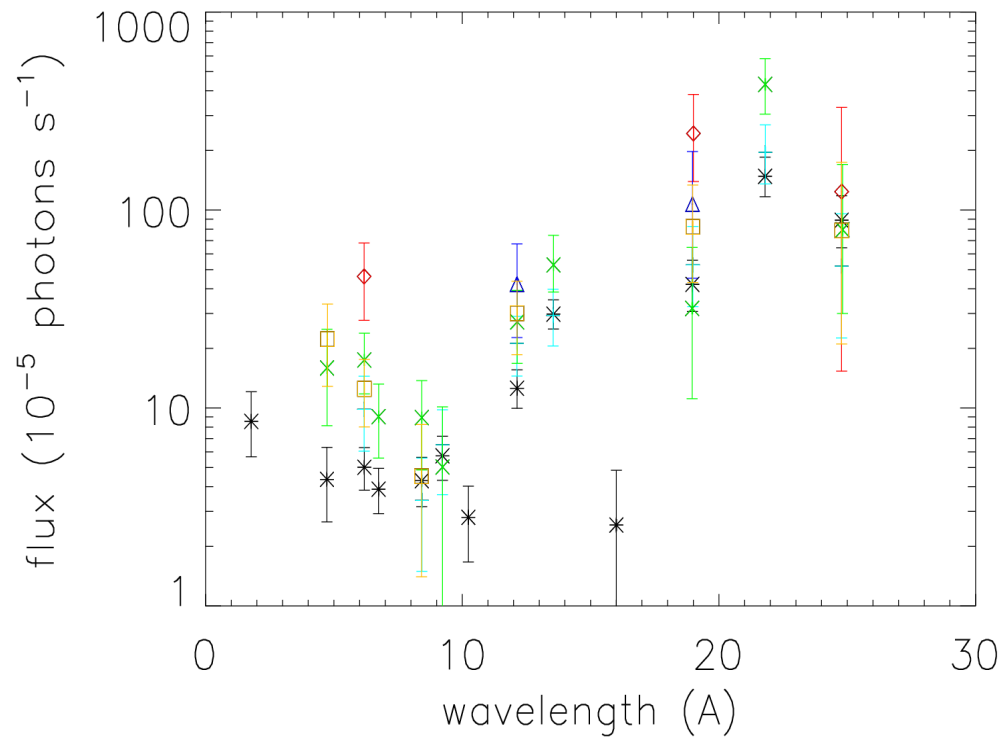


Helium-like triplet lines

Ion	Si XIII	Mg XI	Ne IX	O VII
ID 2749				
$G = \frac{(f+i)}{r}$	$4.277^{+6.619}_{-1.912}$	$4.046^{+3.860}_{-1.609}$	> 7.063	$13.360^{+37.027}_{-7.428}$
$R = \frac{f}{i}$	$3.907^{+7.690}_{-1.823}$	$0.475^{+0.289}_{-0.205}$	$0.093^{+0.086}_{-0.065}$	$0.560^{+0.102}_{-0.054}$
Cash dof	36.1/37	17.4/16	11.2/15	10.4/17
ID 3821				
$G = \frac{(f+i)}{r}$		$4.169^{+119.8}_{-2.474}$	> 3.861	> 2.542
$R = \frac{f}{i}$		$0.719^{+0.921}_{-0.460}$	< 0.375	< 0.480
Cash dof		18.3/23	48.0/17	51.1/18
ID 3822				
$G = \frac{(f+i)}{r}$	> 3.085	> 0.517	> 2.712	> 2.430
$R = \frac{f}{i}$	> 1.832	< 1.408	< 0.289	< 0.262
Cash dof	30.8/40	5.2/13	11.9/12	39.3/16

^aThe line center is fixed at the theoretical value and the line width is fixed as 0.001Å.

Line flux distributions



Resonance Lines (Ly α , Ly β) & Strong i, f lines

Summary

By analysis of six HETGs observations of HerX-1, we found:

- ◆ The continua can be described by a partial covering model which is consistent with the high energy spectra observed with *RXTE*.
- ◆ An additional thermal blackbody component is required to fit the soft band below 12 Å
- ◆ Most spectra show that the strong line emissions from a photoionized accretion disk corona.
- ◆ The strong and variable neutral Fe fluorescence lines are likely associated with the cooler, outer portions of the disk.
- ◆ With the constraints from the triplet lines and line flux distribution, photoionization modelling with *XSTAR* is in progress, which allow us to determine the ionization balance with orbital and superorbital phases.